Commun. Comput. Phys.
doi: 10.4208/cicp.141009.091110s

Vol. **9**, No. 5, pp. 1137-1151
May 2011

Prospective Merger Between Car-Parrinello and Lattice Boltzmann Methods for Quantum Many-Body Simulations

Sauro Succi[1,2,*] and Silvia Palpacelli[3]

[1] *Istituto Applicazioni Calcolo, CNR, via dei Taurini 19, 00185 Roma, Italy.*
[2] *Freiburg Institute for Advanced Studies, Albert-Ludwigs-Universität Freiburg Albertstraβe 19, D-79104 Freiburg i.Br., Germany.*
[3] *Numidia s.r.l., via Berna 31, 00144 Roma, Italy.*

Received 14 October 2009; Accepted (in revised version) 9 November 2010

Available online 14 January 2011

Abstract. Formal analogies between the Car-Parrinello (CP) ab-initio molecular dynamics for quantum many-body systems, and the Lattice Boltzmann (LB) method for classical and quantum fluids, are pointed out. A theoretical scenario, whereby the quantum LB would be coupled to the CP framework to speed-up many-body quantum simulations, is also discussed, together with accompanying considerations on the computational efficiency of the prospective CP-LB scheme.

PACS: 31.15.-p, 47.11.-j
Key words: Quantum many-body problems, Car-Parrinello ab-initio molecular dynamics, lattice Boltzmann method.

1 Introduction

Most successful methods in computational physics usually result from a clever resonance between physical intuition and mathematical transparency. This is certainly the case for the celebrated ab-initio molecular dynamics Car-Parrinello method (CPMD), which combines a very elegant field-theoretically modified Lagrangian with the mathematical/computational principles of dynamical optimization [1]. The result is the "magic" capability of tailoring the dynamic optimization in such a way that the fictitious dynamics of the electronic degrees of freedom leaves them on the desired Born-Oppenheimer surface associated with the actual ionic position at the end of the optimization procedure. This spawns a dramatic boost in the capabilities of computer simulation of molecular system including the electronic degrees of freedom (*ab initio*), which has taken the

*Corresponding author. *Email addresses:* succi@iac.rm.cnr.it (S. Succi), silviapalpacelli@gmail.com (S. Palpacelli)

solid state community by storm for the last 25 years. Although on a very different domain, fluid-dynamics, the lattice Boltzmann method also offers a remarkable example of a powerful combination of physical intuition and mathematical transparency. The main idea of LB is to formulate hydrodynamics in terms of minimal Boltzmann kinetic equation, in which the dynamics of the fictitious molecules (populations) consists of a simple sequence of free-streaming and local relaxation on a regular lattice [2]. The main advantages over standard discretization of the partial differential equations of continuum fluid mechanics (Navier-Stokes) are space-time locality, easy handling of highly irregular boundaries, transparent inclusion of mesoscopic physics beyond the realm of continuum hydrodynamics. Rather than boosting the CFD frontier by orders of magnitude, the LB has greatly facilitated the simulation of an amazingly broad spectrum of fluid-related problems, ranging from the numerical simulation of turbulent flows of industrial relevance, all the way down to the multiscale translocation of biopolymers across biological membranes [3], and lately extended also to quantum and relativistic fluids [4].

The goal of this paper is twofold. First, we wish to point out a few mathematical analogies between CP and LB, which are well rooted into the physics of the problems dealt with by the two methods. Second, we venture on a speculative ground, and envisage a way of putting the LB technique at work to speed-up CP calculations. Although the viability of such speculative thoughts can only be judged by actual practice, we hope that the present considerations may offer a useful guideline for future development of combined CP-LB schemes.

2 Density functional theory for electronic structure simulation

The ab-initio calculation of the energy levels of molecules, including the self-consistent electronic configuration, requires the solution of the N-body Schrödinger equation. Unfortunately, this equation is literally untractable using conventional grid-discretization methods, the blocking hurdle being memory demand: encoding the N-body quantum wavefunction on a spatial grid with L^3 grid points, requires L^{3N} variables. The result is that even small molecules with, say $N=10$ atoms, on a mere $L=10$ grid points per linear dimension, would entail a totally unfeasible (10^{30}) number of variables. The infamous curse of dimensionality.

Fortunately, back in the early 60's, Kohn and Hoenberg were able to show that the molecular ground state is unambiguously fixed by the total electron density $n(\vec{r})$, i.e., a *single* scalar field [5, 6]. This result paved way to effective one-body techniques for electronic structure calculations, i.e., the celebrated Kohn-Sham equations for the electronic orbitals, $\psi_k(\vec{r})$,

$$H_{KS}[n;R_I]\psi_k = E_k\psi_k, \tag{2.1}$$

where $H_{KS}[n;R]$ is the effective Kohn-Sham Hamiltonian, which depends on the total electron density $n(\vec{r}) = 2\sum_k |\psi_k|^2(\vec{r})$, as well as on the set of nuclear (ions) coordinates, here denoted collectively by the symbol R_I.

Since nuclei are much heavier than electrons, their dynamics is typically described by Newton classical equations of motion:

$$M_I \ddot{\vec{R}}_I = -\frac{\partial E[n;R_I]}{\partial \vec{R}_I}, \tag{2.2}$$

where $E[n;R_I]$ is the ion-ion and ion-electron interaction energy, to be detailed shortly. The computational scheme proceeds by advancing the nuclei according to the classical equation of motion (2.2), and then, for each nuclear configuration $\vec{R}_I(t)$, solve the non-linear eigenvalue problem presented by the KS equations.

Although no longer intractable, this still is a very demanding computational task, and consequently alternative solutions strategies are in constant demand.

A particularly attractive option is offered by *dynamic minimization* methods, whereby the KS ground-state is attained as a fixed-point of a fictitious-time dynamics of the orbitals. The simplest such dynamics is given by the steepest-descent (SD) rule

$$\partial_t \psi_k = -\frac{\delta E}{\delta \psi_k^*} = H_{KS}\psi_k. \tag{2.3}$$

It is readily checked, that this is nothing but a one-body Schrödinger equation in imaginary time. That is, rather than solving a set of N simultaneous KS equations, one advances in (imaginary) time an initial set of wavefunction $\psi_k(\vec{r};t=0)$, knowing that, as time unfolds, under the effect of the KS Hamiltonian, all the components of the initial wavefunctions orthogonal to the ground state will eventually annihilate out.

Dynamic techniques are computationally appealing because the system of equations is advanced explicitly in time, with no need of solving simultaneous constraints, i.e., no need of matrix solvers. These matrix-free methods are in principle much more efficient than non-linear eigenvalue solvers, as long as a reasonably fast convergence can be secured. To this purpose, many variants of the simple-minded, first-order SD dynamics have been proposed in the literature, such as higher-order time procedures, Conjugate-Gradient minimization and others.

The Car-Parrinello method stands out as a distinguished member of this class, with a few specific connotations which set it apart for its elegance and physical poignance. In the next section we shall brief revisit the main ideas behind this method.

3 The Car-Parrinello method

The distinguishing feature of the CP scheme is that the functional to be minimized in order to attain the electronic ground state takes the form of an over-arching Lagrangian, keeping both ionic and electronic degrees of freedom under the same umbrella.

The CP Lagrangian reads as follows [1]:

$$L_{CPMD} = \sum_I \frac{M_I}{2}(\dot{\vec{R}}_I)^2 - E[\psi_k,\vec{R}_I] + 2m_e\sum_k |\dot{\psi}_k|^2 + 2\sum_{kl}\Lambda_{kl}(\psi_{kl}-\delta_{kl}),$$

where $I=1,N_I$ runs over the number of ions and $k=1,N_{orb}$ over the number of occupied orbitals. In the above, M_I are the ionic masses, m_e the (fictitious) electronic ones, $\psi_{kl}\equiv\int\psi_k^*(\vec{r})\psi_l(\vec{r})d\vec{r}$, and Λ_{kl} are Lagrangian parameters enforcing the orthogonality constraints. The functional $E[\psi_k,\vec{R}_I]$ describes the potential energy surface, defined by the following expression:

$$E=\frac{1}{2}\sum_{I>J}\frac{Z_IZ_J}{|\vec{R}_I-\vec{R}_J|}+E_{xc}[n]+\frac{1}{2}\int d\vec{r}d\vec{r'}\frac{n(\vec{r})n(\vec{r'})}{|\vec{r}-\vec{r'}|}$$
$$-\sum_k\psi_k^*(\vec{r})\Delta\psi_k(\vec{r})d\vec{r}+\int V_{ext}(\vec{r})n(\vec{r})d\vec{r}, \tag{3.1}$$

where Z_I is the ionic charge, $n(\vec{r})=2\sum_k|\psi_k(\vec{r})|^2$ is the total electron density, $V_{ext}(\vec{r})$ is an external potential and E_{xc} is the exchange energy, typically a local functional of the form $E_{xs}[n]=const\cdot\int n^{1/3}(\vec{r})d\vec{r}$.

The novelty of the over-arching CP Lagrangian is that electronic degrees of freedom (electron orbitals) are treated as extended Newtonian variables. As a result, the minimization dynamics takes the form of Euler-Lagrange equations for both the ionic coordinates and the orbital wavefunctions, i.e.,

$$\frac{\delta L_{CP}}{\delta\vec{R}_I}-\frac{d}{dt}\frac{\delta L_{CP}}{\dot{\vec{R}}_I}=0,\quad\text{and}\quad\frac{\delta L_{CP}}{\delta\psi_k^*}-\frac{d}{dt}\frac{\delta L_{CP}}{\dot{\psi}_k^*}=0,$$

where $\dot{\psi}_k\equiv\partial_t\psi_k$.

In Newtonian form, these read as follows:

$$M_I\ddot{\vec{R}}_I=-\frac{\partial E[R,n]}{\partial\vec{R}_I},$$
$$m_e\ddot{\psi}_k=-\frac{1}{2}\frac{\delta E[n,R]}{\delta\psi_k^*}+\sum_l\Lambda_{kl}\psi_l.$$

More explicitly,

$$m_e\ddot{\psi}_k=\Big\{-\frac{\hbar^2}{2m}\Delta+V_{ext}+V_H+V_{xc}\Big\}\psi_k+\Lambda_k,$$

where

$$V_H(\vec{r})=\int\frac{n(\vec{r'})}{|\vec{r}-\vec{r'}|}d\vec{r'}$$

is the long-range Hartree potential and $\Lambda_k=\sum_l\Lambda_{kl}$.

The magic point is that the fictitious motion of the electronic degrees of freedom, from say, t to $t+\Delta t$, lands them exactly on the Born-Oppenheimer surface associated with the actual ionic position at time $t+\Delta t$. As a result, the CP dynamics is such that, by the time the electrons are landed to their KS ground state, the nuclear ions have also moved to their correct (i.e., consistent with the actual electronic configuration) positions! This is why the CP method sticks out among all dynamic minimization techniques, as a "unified" molecular dynamics, including electronic degrees of freedom.

4 Lattice Boltzmann

Next we discuss the second method of the analogy, namely the lattice Boltzmann technique.

The lattice Boltzmann equation (LBE) is a minimal form of Boltzmann kinetic equation which is meant to simulate the dynamic behavior of fluid flows without directly solving the equations of continuum fluid mechanics. Instead, macroscopic fluid dynamics emerges from the underlying dynamics of a fictitious ensemble of particles, whose motion and interactions are confined to a regular space-time lattice. The lattice Boltzmann equation reads as follows [2]:

$$f_i(\vec{r}+\vec{c}_i dt, t+dt) = f_i(\vec{r};t) + \Omega_{ij}\, dt\left(f_j^{eq}(\vec{r};t) - f_j(\vec{r};t)\right). \tag{4.1}$$

In the above $f_i(\vec{r};t)$ represents the probability of finding a particle at position $\vec{r}$ and time t with velocity $\vec{c}_i$. Here, the subscript i labels a set of discrete speeds connecting the nodes of a regular lattice. Repeated indices are summed upon. The right hand side of Eq. (4.1) corresponds to an *exact* discrete-velocity representation of the Boltzmann streaming operator $\partial_t f + \vec{v}\cdot\nabla f$, while the right-hand side stands for particle-collisions, represented through a relaxation to a local equilibrium. Such relaxation is controlled by the scattering matrix Ω_{ij}, whose eigenvalues define the relaxation time-scale. The local equilibrium f_i^{eq} is the lattice analogue of a local Maxwellian with density $\rho = \sum_i f_i$, and flow velocity $\vec{u} = \sum_i f_i \vec{c}_i/\rho$ (see below). In practical applications, such matrix is often taken in its simplest, diagonal form, resulting in the so called Lattice BGK (LBGK) scheme [7], after the continuum mode Boltzmann equation introduced by Bhatnagar-Gross-Krook, back in 1954 (see [8]). The discrete local equilibria are typically given by a second-order expansion in the Mach-number of a local Maxwellian,

$$f_i^{eq}(\vec{v};t) = w_i\rho\left(1 + \frac{u_a c_{ia}}{c_s^2} + \frac{u_a u_b Q_{iab}}{2c_s^4}\right), \tag{4.2}$$

where w_i is a set of weights normalized to unity, and $Q_{iab} = c_{ia}c_{ib} - c_s^2\delta_{ab}$ is the quadrupole projector along the i-th direction, and $c_s^2 = kT/m$ is the sound speed, defined as $c_s^2 = \sum_i w_i c_i^2/D$, D being the number of spatial dimensions. In the above, subscripts denote cartesian components, and repeated indices are summed upon. The reason for expanding to second order in the flow field, more precisely in the local Mach-number $Ma = u/c_s$, is related to the lack of symmetry of a given lattice to ensure the isotropy of higher tensors coupling to higher powers of the Mach-number. Fortunately, isotropy of fourth-order tensors $T_{abcd} = \sum_i c_{ia}c_{ib}c_{ic}c_{id}$, is sufficient to recover the correct behavior of low-Mach, quasi incompressible flows. More demanding applications, with major thermal/compressibility effects, call for higher-order lattices. Once the discrete populations f_i are known, the main fluid quantities are obtained by simple (linear) summation upon the discrete speeds,

namely

$$\rho(\vec{r};t)=\sum_{i=0}^{b} f_i(\vec{r};t), \quad \rho(\vec{r};t)\vec{u}(\vec{r};t)=\sum_{i=0}^{b} f_i(\vec{r};t)\vec{c}_i, \quad \text{and} \quad \vec{\vec{P}}(\vec{r};t)=\sum_{i=0}^{b} f_i(\vec{r};t)\vec{c}_i\vec{c}_i,$$

for the fluid density, current, and momentum flux tensor (particle mass made unit for simplicity). It should be appreciated that, while ρ and $\rho\vec{u}$ are conserved quantities, only the trace of the momentum-flux tensor is conserved, which corresponds to the fluid kinetic energy (pressure). The non-diagonal components of $\vec{\vec{P}}$ are zero at equilibrium, and represent the fluid shear

$$\vec{\vec{S}}=\frac{1}{2}(\nabla\vec{u}+\vec{u}\nabla).$$

Chapman-Enskog analysis of the LBE shows that in the limit of long-wavelengths, low-frequency, the Eq. (4.1) reproduces exactly the Navier-Stokes equation for quasi-incompressible flows, with an ideal equation of state $P=\rho c_s^2$, and a kinematic viscosity $\nu=c_s^2(\tau-\Delta t/2)$, τ being the leading non-zero (inverse) eigenvalue of the matrix Ω and $kT/m=c_s^2$ the fluid temperature. The conceptual and practical simplicity of this scheme lie at the heart of the computational efficiency of the LBE, and form a solid basis for its success as a Navier-Stokes simulator "in kinetic disguise". The main computational highlights of LB are now fully appreciated, namely: i) Non-locality (streaming) is linear and non-linearity (collision) is local. This should be contrasted with Navier-Stokes equations, in which the transport term $u\nabla u$ is non-local and non-linear at a time. In particular, this terms shows that the fluid momentum is transported along the material streamlines $d\vec{r}=\vec{u}dt$, defined by the fluid velocity itself. For complex flows, such streamlined can become very "wild" and demanding in terms of numerical stability; ii) Streaming is *exact*, since it proceeds along constant streamlines $d\vec{r}_i=\vec{c}_i dt$ (light-cones); iii) Complex boundary conditions are easily formulated in terms of elementary mechanical rules (bounce-back, reflections) of interactions of the LB 'molecules' with solid walls; iv) Fluid pressure and the strain tensor are available locally, on-the-fly, as linear combinations of the equilibrium and non-equilibrium components of the discrete distribution function, respectively. This means that pressure can be obtained from the flow field configuration with no need of solving a (usually very expensive) Poisson problem; v) Nearly ideal amenability to parallel computing (low communication/computation ratio). These aspects configure LB as a very special finite-difference scheme for hydrodynamics and lie at the heart of its impressive growth as an alternative numerical technique for complex fluid dynamic problems.

5 CP-LB analogies

The CP and LB method do exhibit a few formal analogies, at both methodological and conceptual levels. In the following, we shall briefly illustrate them.

5.1 Acceleration by magnification of small parameters

Both CP and LB boost their computational efficiency through artificial magnification of a smallness parameter controlling the size of the time step. For CP, this is the ratio of the electronic to ionic mass, while for LB it is the Mach number, i.e., the ratio of the fluid to sound speed velocity. As we shall see, both come to the same. The general principle is quite familiar in computational physics: if the scope is to go from A at time t_A to B at time $t_B > t_A$, it is not necessary to follow the actual physical trajectory, but one is free to choose the most convenient fictitious one sharing with the physical one just the extremals A and B. This is generally achieved by boosting a suitable smallness parameter, associated with the time-marching procedure.

In the CP method, $\epsilon = m_e/M_I$, is typically artificially boosted by several orders of magnitude [9, 10], thereby permitting a corresponding increase of the electronic time-step. This is fine, as long as the magnified time-step is still able to keep the electrons sufficiently close to the adiabatic Born-Oppenheimer energy surface.

A similar applies to the Mach number $Ma = U/c_s$ in LB simulations. Low Mach numbers tax the LB timestep on account of the fact that the simulation span is inversely proportional to the average fluid speed, $T = L/U$, L being the typical linear size of the simulation box and U a typical flow speed. Since LB is weakly compressible, it comes with compressibility errors of the order Ma^2. Slow flows, say in porous media, feature Mach numbers well below 10^{-4}, with correspondingly long simulation time, if sound motion is to be explicitly tracked. However, since compressibility errors scale like Ma^2, enhancing the Mach number to, say, $Ma = 0.1$ would result in a thousand times shorter simulation time, with a compressibility error of the order 0.01, which is often tolerable for practical purposes.

Therefore, by boosting the fluid velocity U and/or reducing the sound speed c_s, the time-step can be significantly increased, without compromising the physical observables of interest.

The CP-LB analogy can be made even sharper, by observing that the fictitious electronic mass m_e in the CP equations has the dimension of mass per length square, so that one can define an electronic sound speed as $\hbar/\sqrt{mm_e}$. This formally shows that raising m_e is equivalent to lowering the sound speed, precisely like in LB.

5.2 Space and time on the same footing

A second, perhaps more profound analogy, between CP and LB, is the fact of replacing an unbalanced space-time formalism with a balanced one. For CP, this means moving from the standard Schrödinger like Kohn-Shan formalism (first order in time, second in space) to the Klein-Gordon context, which is second order in both space and time. As shown in the previous section, the fictitious electron mass in front of the second order time derivative defines a fictitious electronic sound speed which is made much smaller than the physical one, so as to allow correspondingly larger time-steps.

Aside from this acceleration trick, however, the point of the second-order formalism is to allow the introduction of a formally unified Lagrangian collecting both ionic and electronic degrees of freedom.

The LB works on a fairly similar philosophy. Indeed, it replaces the hydrodynamic Navier-Stokes equations (first order in time, second in space) with the hyperbolic Boltzmann kinetic equation, first order in both space-time. Here the move is not fictitious, in that kinetic theory is a physical uplift of hydrodynamics from configuration space to phase-space.

For the LB case, such balanced first-order dynamics brings about a number of significant advantages, primarily the fact that the time-step scales linearly with the mesh-spacing, rather than quadratically as in ordinary explicit grid-methods, thereby avoiding the time-step "collapse" as the grid spatially refined.

For the CP case, besides the conceptual advantage of casting the minimization problem in terms of a physical Lagrangian, it is observed that the second-order dynamics in time allows the CP scheme to converge to the ground state from "both sides", i.e., via damped oscillations rather than one-sided monotonic damping. Some authors argue that is beneficial to the numerical stability of the CP scheme, although the argument appears to be still open to debate.

6 Quantum lattice Boltzmann

The LB-CP analogies discussed so far highlight some cute commonalities between two successful methods, each however on its own separate domain. Hence, they do not bear directly upon a possible merge upon the two techniques.

An interesting question arises as to whether LB techniques/ideas could be embedded within the CP framework, so as to speed-up quantum many body calculations. To this end, a quantum version of LB is clearly a pre-requisite. The good news is that such quantum LB schemes are indeed available in the current literature [11–14], so that the task appears technically feasible, at least in principle.

The quantum LB (QLB) starts from the Dirac equation in Maiorana form [15]:

$$\partial_t \Psi_i + A^a_{ij} \partial_a \Psi_j = \Omega_{ij} \Psi_j, \tag{6.1}$$

where $\Psi_i, i=1,4$ is the complex Dirac 4-spinor, A^a, $a=x,y,z$ are the Dirac-Maiorana advection matrices, and Ω is the mass/collision matrix. Note the Maiorana form of the Dirac equation is chosen, for in this case all matrices are real, thereby stressing the analogy to a classical Boltzmann equation. The detailed form of these matrices is given in [15]. Here, we only remark that the major departure from a classical Boltzmann equation is that only one of the three advection matrices can be diagonal at a time, with eigenvalues $(1,1,-1,-1)$, corresponding to classical motion of two walkers, moving along opposite directions, say $\pm z$, if the matrix A^z is chosen to be diagonal. This is because Dirac spinors mix in spinor space as they propagate, so they cannot be treated as classical movers in

more than one spatial dimension. The starting point of the QLB is to identify the spinorial index with a discrete speed, and treat the Dirac equation just as an ordinary discrete Boltzmann equation for a complex distribution function Ψ_i. In one-dimension, the game is easy: the diagonal streaming operator can be advanced exactly in time along the light-cone, $dz=\mp cdt$, and the r.h.s. can be treated as an ordinary collision operator. Crank-Nicholson time-marching delivers the following compact QLB [13, 14]:

$$\Psi_i(z,t+dt)=T_{ij}\Psi_j(z-c_j dt,t), \tag{6.2}$$

where $c_j=\mp 1$, and the transfer matrix is $T_{11}=T_{22}=\cos\theta$, and $T_{12}=-T_{21}=\sin\theta$, where $\cos\theta=(1-m^2/4)/(1+m^2/4)$, $m\equiv\omega_c dt$, ω_c being the Compton frequency. Note that the matrix T is unitary for any size of the timestep dt. By denoting with u and d the bispinors propagating upwards and downwards respectively in $d=1$, it is readily checked that the Dirac equation reduces to a relativistic Klein-Gordon equation

$$\partial_{tt}\psi-c^2\partial_{xx}\psi=-\omega_c^2\psi,$$

where $\psi=u,d$. The non-relativistic Schrödinger dynamics is shown to descend from the relativistic one upon adiabatic enslaving of the fast mode, $\Phi^-=e^{imc^2t}(u-id)/\sqrt{2}$, to the slow one, $\Phi^+=e^{-imc^2t}(u+id)/\sqrt{2}$. Under the adiabatic condition $|\partial_t\Phi^-|<2\omega_c|\Phi^-|$, the QLB naturally reduces to the non-relativistic Schrödinger dynamics.

The extension to particles of charge q, interacting with a vector potential $A(z)$, is easily accommodated by noting that the well-know correspondence rule $p\to p+iqA$, just translates into charge dependent mass term (here q is the electronic charge).

For the simple case of a static potential $V(z)$:

$$T_{11}=T_{22}=\frac{1-M^2/4}{1+M^2/4-ig},$$
$$T_{12}=-T_{21}=\frac{m}{1+M^2/4-ig},$$

where $g=qV(z)/mc^2$ is the coupling strength, and $M^2\equiv m^2-g^2$.

6.1 Ground-state calculations

The real-time QLB formalism is readily turned to imaginary-time for ground state calculations. Essentially, the usual Wick rotation from real to imaginary time, $t\to it$, is equivalent to an analogue mass/frequency rotation, $\omega_c\to i\omega_c$, in real time. Since the QLB formalism deals with complex variables anyway, one can seamlessly Wick-rotate the mass/frequency while leaving time real. As a result, periodic oscillations are turned into decaying exponentials, so that excited states are projected out in the course of the evolution, leaving the ground state as a time-asymptotic wavefunction. Ground state calculations using QLB have been demonstrated in [16].

6.2 Multi-dimensional QLB

Multidimensional extensions of QLB to $d>1$ are non-trivial.

The QLB strategy to cope with dimensionality issues consists of diagonalizing A^z, A^y, A^x one at a time and advance the spinors along z,y,x respectively through an operator splitting at each step. This way, the 3d problem is advanced as a sequence of three one-dimensional ones, each of which keeps the spin aligned with the velocity vector. Formally, the 3d QLB propagator reads as

$$T_{xyz}=(R_x^{-1}P_xR_x)(R_y^{-1}P_yR_y)P_z,$$

where R_y and R_x are rotation matrices which the spin aligned with the axis y and x, during the propagation along y and x, respectively. In the above, $P_a=\exp[(D^a+\Omega^a)dt/3]$ is the propagator along direction $a=x,y,z$. Note that at each step, the streaming matrix A^a takes a diagonal form D^a with eigenvalues ±1 along direction $\pm x_a$. Very recently, the scheme has been shown to produce second-order accurate results also for the relativistic Dirac wave equation [17].

In two dimensions, the procedure is found to provide satisfactory results [16, 18].

In three dimensions, significant isotropy errors were reported [16], which have been fixed only very recently. In a forthcoming publication [19], a detailed analysis of the isotropy of the three-dimensional model is presented and the scheme shown to recover isotropy within a discretization error which is found to scale linearly with the mesh resolution.

Here we only show preliminary results for a very simple test case, demonstrating the recovery of isotropy: a Gaussian wave packet, which is let free to expand following the Schrödinger equation (i.e., no external potential is applied). In this case, the analytical solution of the Schrödinger equation is well known, and in particular, the mean spread evolves according to the following equation along each axis direction:

$$\Delta_a(t)=\sqrt{\Delta_0^2+\frac{\hbar^2t^2}{4m^2\Delta_0^2}},\qquad a=x,y,z, \tag{6.3}$$

where Δ_0 is the initial spreading of the wave packet.

As an example of a recent 3d application of QLB in real-time (stand-alone, no coupling to CP), in Fig. 1 we show the measured spreads for a free particle with $m=0.35$ and $\Delta_0=14$. The simulation is performed in a cube with side length 100, using 100^3 nodal points. From Fig. 1, a good agreement between the three spreads is observed and also with the Schrödinger solution of Eq. (6.3).

We then refined the lattice by using 200^3 and 300^3 nodal points and in Fig. 2, we show the evolution of the mean difference between spreads normalized dividing by the analytical value given in Eq. (6.3) for the three lattices. As one can see, the mean difference tends to decrease under grid refinement.

The oscillations in the initial transient are attributed to non-adiabatic effects, holding memory of the initial condition. It is also observed that the deviation of the QLB result

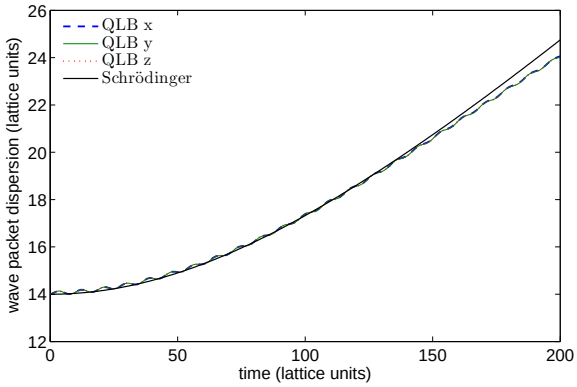

Figure 1: Dispersion of a wave packet with initial spread $\Delta_0=14$, mass $m=0.35$ and no potential. Computed spreads Δ_x, Δ_y and Δ_z versus the Schrödinger solution of Eq. (6.3) are shown. The grid size is 100^3 nodal points.

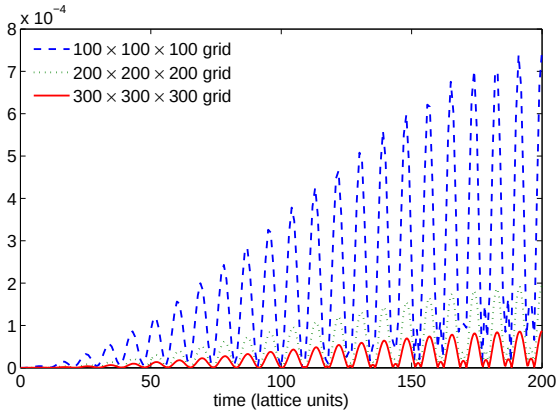

Figure 2: Evolution of the average of $|\Delta_x-\Delta_y|$, $|\Delta_x-\Delta_z|$ and $|\Delta_y-\Delta_z|$ (in lattice units), for a wave packet with initial spread $\Delta_0=14$, mass $m=0.35$ and no potential. The average values are normalized dividing by the analytical value of the spread, as given by Eq. (6.3). Results are computed for three lattices of sizes 100^3, 200^3 and 300^3 discretizing a cube with side length 100.

from the analytical solution, amounts to a few percent after a few hundred time-steps. As recently shown by Dellar and coworkers, [20], such deviations are due to the fact that, also in the long-term, the QLB results stay closer to the solution of the Dirac equation than to the Schrödinger dynamics. This might be a problem for the prospective CP-LB coupling, which requires adiabaticity of the electrons around the Born-Oppenheimer energy surface.

On the other hand, one should bear in mind that the CP-LB merge would concern mainly ground-state calculations, hence operate with the imaginary-time version of QLB, in which case non-adiabatic effects are set to damp out as imaginary-time unfolds. Examples of (fourth-digit) accurate ground-state QLB calculations of the two-dimensional Gross-Pitaevskii equation can be found in [21].

However, only actual practice can tell whether non-adiabaticity errors can be kept to sufficiently small for the accuracy required in quantum-many ground-state simulations.

7 Coupling QLB to CP

Having discussed the QLB scheme in dimension $d=1,2,3$, we next move on to investigate whether QLB could be used in the context of quantum many body problems, and particularly in connection with the CP method.

Since Density Functional Theory casts the quantum N-body problems in terms of N effective one-body problems, i.e., the Kohn-Sham equations, it is clear that the most direct use of QLB in this framework would be to serve as a fast KS solver.

To the purpose of realizing a first-order steepest-descent strategy, the QLB can be used in its non-relativistic vests.

Since the CP approach replaces the Schrödinger-form of the KS with a Klein-Gordon-like formulation (second order in space and time), the coupling to CP seems best suited to the non-adiabatic, relativistic form of QLB. In the following, we discuss the prospective changes/extensions which are required to fulfill the task, at least in principle.

7.1 Non-linear coupling via the electron density

The QLB scheme involves a spinor ψ_{jk} for each electron orbital k, all orbitals being coupled through the overall density $n(\vec{r})$. Leaving aside for the moment the Hartree interactions, the corresponding non-linearities are local, hence similar to the one presented by the Gross-Pitaevskii equation, which has been solved before by QLB techniques [16]. Hence, in principle, this does not seem to pose any new difficulty.

In practice, one would advance all orbitals in parallel, synchronize and collect the global density $n(\vec{r})$ and compute all relevant density-dependent interactions for the next step.

7.2 Long-range interactions

Long-range Coulombic interactions, as represented by the Hartree term in the KS Hamiltonian, are known to be computationally demanding, and especially challenging for parallel implementations since they carry an all-to-all coupling. This problem is generally handled by casting these interactions in the form a Poisson equation for the Hartree potential, i.e.,

$$\Delta V_H(\vec{r}) = n(\vec{r}). \tag{7.1}$$

To preserve the explicit (matrix-free) nature of both LB and CP, such Poisson problem can be solved through some form of fictitious time-marching iterative procedure.

7.3 Orthogonality constraints

The next feature are the orthogonality constraints. Given that the Lagrangian parameters Λ_{kl} need to be computed on the fly, *once available*, they enter the QLB equation in a very simple form, i.e., a linear term, simply adding to the collision matrix $\Omega_{ij,kl}\psi_{j,l}$. Of course, the whole machinery to keep the orbitals orthogonal throughout, which involves substantial matrix algebra, would stay untouched. In this respect, QLB, as-is, would not bring any specific advantage to the current CP technology, which is unfortunate because orthogonalization is the major computational bottleneck of the CP procedure.

7.4 Coupling to nuclear motion

Finally, coupling to the nuclear motion can be handled again at the level of the collision matrix, which picks up a dependence on the actual ionic positions $\vec{R}_I(t)$. Here, the procedure could borrow much from existing multiscale version of LB, coupling classical fluids to (charged) colloidal particles [22, 23]. The long-range ion-ion interactions could again be solved via a particle-mesh Poisson solver for the nuclear motion.

Summarizing, none of the specific quantum interactions appearing in the Kohn-Sham Hamiltonian/Car-Parrinello Lagrangian, seems to raise a no-go to the prospective use of QLB as a quantum many-body accelerator. Conceptually, all steps above seem to be compatible with the QLB structure, as we know it, once the effective potential V is made a suitable function(al) of the electron density $n(\vec{r})$ and nuclear coordinates $\vec{R}_I(t)$. However, new ideas are required in order to speed-up the orbital orthogonalization procedure.

8 Computational considerations

Having shown that the merger between CP and LB appears to be viable, at least in principle, the next question is: what advantages can we draw from it? More precisely, what LB assets for classical fluids would eventually carry on to the quantum CP context?

Earlier versions of CP were based on plane-wave expansions of the electron orbitals, i.e., the well-known spectral method, the technique of choice for calculations in periodic domains. LB simulations of homogeneous turbulence have shown comparable accuracy and efficiency as spectral methods (the golden standard for periodic homogeneous computations), with recent results advocating substantial advantages upon using higher-order discrete velocity stencils [24]. The major advantage of LB versus spectral methods is twofold: first, LB is by no means restricted to periodic geometries; second, LB lends itself to highly efficient parallel implementations, both in simple [25] and quite complex geometries [26].

Modern CP simulations make use of localized basis functions for the electron orbitals, designed in such a way as to cluster the numerical grid around the nuclear positions, where the electron orbitals tend to localize. This calls for non-uniform, and possibly adaptive, real-space techniques. LB versions with non-uniform, or even adaptive grid

refinement, are available in the LB literature [27]. Inevitably, these advanced LB versions are significantly more complex and computationally-demanding than the standard cartesian LB formulation.

Another consideration regards the time-stepping procedure.

In the LB formalism, diffusion (kinetic energy in the CP framework) emerges from adiabatic relaxation of the fast modes to the slow ones, with no need of second order spatial derivatives. This means that the time-step scales only linearly with the mesh size, at variance with most explicit grid methods, in which the time-steps scales quadratically with the grid-size, thus rapidly leading to unacceptably small times-steps as the grid is refined. Exactly the same mechanism applies to QLB, in which the non-relativistic Schrödinger equation emerges from adiabatic enslaving (in imaginary time) of the fast mode Φ^- to the slow one, Φ^+. Based on the above, it is plausible to expect that the main benefits of LB philosophy for classical fluids, i.e., very large lattices, each lattice site requiring a lean amount of computation and very little communication, might prove beneficial to the CP context as well.

Summarizing, we believe that the main potential advantages of the prospective CP-LB merger are as follows: parallel efficiency, eventually in combination with non-trivial geometries, and large time-steps, as long as non-adiabaticity errors can be kept under control.

9 Conclusions

Summarizing, we have discussed some analogies between the Car-Parrinello ab-initio molecular dynamics for quantum molecules, and the Lattice Boltzmann method for classical and quantum fluids. While the analogies with the classical LB remain at a somewhat formal level, quantum LB techniques might bear some concrete value for quantum many-body simulations based on density functional theory. To this regard, a theoretical scenario has been envisaged, whereby QLB could be coupled together with CP for realistic quantum many-body simulations. A few considerations on the computational efficiency of the prospective CP-LB scheme have also been presented. Whether the theoretical scenario portrayed in this paper will ever turn into a practical new-entry in the family of computational methods for quantum many-body systems, only future (simulations) can tell.

References

[1] R. Car, and M. Parrinello, Unified approach for molecular dynamics and density-functional theory, Phys. Rev. Lett., 55 (1985), 2471–2474.

[2] R. Benzi, S. Succi, and M. Vergassola, The lattice Boltzmann equation: theory and applications, Phys. Rep., 222 (1992), 145–197.

[3] S. Succi, Lattice Boltzmann across scales: from turbulence to DNA translocation, Euro. Phys. J. B., 64 (2008), 471–479.

[4] M. Mendoza, B. M. Boghosian, H. J. Herrmann, and S. Succi, Fast lattice Boltzmann solver for relativistic hydrodynamics, Phys. Rev. Lett., 105 (2010), 014502.
[5] P. Hohenberg, and W. Kohn, Inhomogeneous electron gas, Phys. Rev., 136 (1964), B864–B871.
[6] W. Kohn, and L. J. Sham, Self-consistent equations including exchange and correlation effects, Phys. Rev., 140 (1965), A1133–A1138.
[7] Y. H. Qian, D. D'Humieres, and P. Lallemand, Lattice BGK models for Navier-Stokes equation, Europhys. Lett., 17 (1992), 479–484.
[8] P. L. Bhatnagar, E. Gross, and M. Krook, A model for collision processes in gases. I. small amplitude processes in charged and neutral one-component systems, Phys. Rev., 94 (1954), 511–525.
[9] M. Tuckerman, and M Parrinello, Integrating the Car-Parrinello equations I. basic integration techniques, J. Chem. Phys., 101 (1994), 1302–1315.
[10] M. Tuckerman, and M Parrinello, Integrating the Car-Parrinello equations II. multiple time-scale techniques, J. Chem. Phys., 101 (1994), 1316–1329.
[11] B. M. Boghosian, and W. Taylor, Quantum lattice-gas model for the many-particle Schrödinger equation in d dimensions, Phys. Rev. E., 57 (1998), 54–66.
[12] J. Yepez, and B. M. Boghosian, An efficient and accurate quantum lattice-gas model for the many-body Schrodinger wave equation, Comput. Phys. Commun., 146 (2002), 280–294.
[13] S. Succi, and R. Benzi, Lattice Boltzmann equation for quantum mechanics, Phys. D., 69 (1993), 327–332.
[14] S. Succi, Numerical solution of the Schrödinger equation using discrete kinetic theory, Phys. Rev. E., 53 (1996), 1969–1975.
[15] L. Landau, and E. Lifshitz, Relativistic Quantum Field Theory, Pergamon, Oxford, 1960.
[16] S. Palpacelli, and S. Succi, The quantum lattice Boltzmann equation: recent developments, Commun. Comput. Phys., 4 (2008), 980–1007.
[17] P. Dellar, and D. Lapitski, APS March Meeting, Y22012, 2010.
[18] S. Palpacelli, and S. Succi, Numerical validation of the quantum lattice Boltzmann scheme in two and three dimensions, Phys. Rev. E., 75 (2007), 066704.
[19] P. Dellar, D. Lapitski, S. Palpacelli, and S. Succi, in preparation.
[20] P. Dellar, and D. Lapitski, in preparation.
[21] S. Palpacelli, S. Succi, and R. Spigler, Ground-state computation of Bose-Einstein condensates by an imaginary-time quantum lattice Boltzmann scheme, Phys. Rev. E., 76 (2007), 036712.
[22] P. Ahlrichs, and B. Dunweg, Simulation of a single polymer chain in solution by combining lattice Boltzmann and molecular dynamics, J. Chem. Phys., 11 (1999), 8225–8239.
[23] M. G. Fyta, S. Melchionna, E. Kaxiras, and S. Succi, Multiscale coupling of molecular dynamics and hydrodynamics: application to DNA translocation through a nanopore, Multiscale. Model. Simul., 5 (2006), 1156–1173.
[24] S. S Chikatamarla, and I. V. Karlin, Entropy and Galilean invariance of lattice Boltzmann theories, Phys. Rev. Lett., 97 (2006), 190601.
[25] S. Succi, G. Amati, and R. Piva, Massively parallel lattice Boltzmann simulation of turbulent channel flow, Int. J. Mod. Phys. C., 8 (1997), 869–877.
[26] M. Bernaschi, S. Melchionna, S. Succi, M. Fyta, E. Kaxiras, and J. K. Sircar, MUPHY: a parallel multi physics/scale code for high performance bio-fluidic simulations, Comput. Phys. Commun., 180 (2009), 1495–1502.
[27] J. Tölke, S. Freudiger, and M. Krafczyc, An adaptive scheme using hierarchical grids for lattice Boltzmann multi-phase flow simulations, Comput. Fluids., 35 (2006), 820–830.